A R C H I V E S O F M E T A L L U R G Y A N D M A T E R I A L S
Volume 59 2014 Issue 4
DOI: 10.2478/amm-2014-0217

R. BOGUCKI*, K. MOSÓR*, M. NYKIEL*

EFFECT OF HEAT TREATMENT CONDITIONS ON THE MORPHOLOGY OF α PHASE AND MECHANICAL PROPERTIES IN Ti-10V-2Fe-3Al TITANIUM ALLOY

WPŁYW WARUNKÓW OBRÓBKI CIEPLNEJ NA MORFOLOGIĘ FAZY α I WŁASNOŚCI MECHANICZNE W STOPIE TYTANU Ti-10V-2Fe-3Al

The influence of heat treatment on the microstructure and mechanical properties was studied in the Ti-10V-2Fe-3Al titanium alloy for two heat treatment schemes $(\alpha+\beta)$ and $\beta+(\beta+\alpha)$, which resulted in different morphologies of the α phase. Scheme I resulted in the α-phase of globular morphology, whose volume fraction did not change much during annealing. Scheme II led to obtaining a needle-like α-phase, whose amount increased together with heating time. The phenomenon of stress-induced martensitic transformation was observed in the material with needle-like morphology annealed for 15 and 30 min. Longer times of annealing effected in the decay of that transformation, provided the volume fraction of α-phase exceeded 50%.

Keywords: phase transformations, microstructure, mechanical properties, β-phase, α-phase

W pracy przedstawiono wyniki badań wpływu obróbki cieplnej na mikrostrukturę i właściwości mechaniczne stopu tytanu Ti-10V-2Fe-3Al, które analizowano w dwóch schematach obróbki cieplnej $(\alpha+\beta)$ oraz $\beta+(\beta+\alpha)$. Uzyskane mikrostruktury charakteryzowały się różną morfologią fazy α. W schemacie I obserwowano globularną fazę α, której udział objętościowy nie ulegał znacznym zmianom w funkcji czasu wygrzewania. W schemacie II faza α miała kształt iglasty i jej udział objętościowy wzrastał z czasem wygrzewania. W próbkach o iglastej morfologii fazy α dla czasów wygrzewania 15 min. i 30 min. zaobserwowano występowanie zjawiska przemiany martenzytycznej indukowanej naprężeniem. Zastosowanie dłuższych czasów wygrzewania ujawniło zanik dodatkowej.

1. Introduction

Titanium alloys are a great alternative for high-strength structural steels. They have high mechanical properties, good ductility and deformability at a low specific weight. Titanium alloys, depending on the chemical composition, may have the structure of a single α or β phase and two-phase $(\alpha+\beta)$.

The highest mechanical properties are obtained in the alloys of β and pseudo- β structure [1-4], in which the basic elements stabilizing the β structure are V, Mo, Fe, Nb. Generally, the β or $(\alpha+\beta)$ titanium alloys have been widely used in airplane and space industries, while the single α-phase ones have found application as medical implants. The titanium alloys of β structure were used for the first time in the sixties of the last century, when two airplanes Lockheed SR-71 and Blackbird were constructed [5]. Nowadays, the Ti-10V-2Fe-3Al alloy of metastable β structure has been widely used for extremely loaded plane elements. The control of temperature and time of heat treatment enables changing the morphology of α-phase and obtaining required properties in a wide range. The annealing in the $(\alpha+\beta)$ range leads to the formation of globular particles of the α-phase, the volume fraction of which changes in dependence on temperature [6-7]. Heating the alloy up to temperature above the $\alpha \rightarrow \beta$ transformation followed by cooling below the temperature of β-phase stability, brings about the appearance of the α-phase in the form of needles and its amount depends on temperature and time of annealing [6]. It was observed, that the values of volume fractions of α- and β-phases decided on the appearance of strain-induced martensitic transformation SIM [8-10]. Such a transformation occurred, when the volume fraction of α-phase was less than 50% [6]. The SIM studies carried so far focused on the analysis of β-phase grain size and annealing temperature [6, 11-15].

In the present work, the results of examination of the influence of annealing times in the $(\alpha+\beta)$ and $\beta+(\alpha+\beta)$ range on the formation of microstructure and mechanical properties of the titanium alloy of the Ti-10V-2Fe-3Al type have been shown.

2. Experimental procedure

The Ti-10V-2Fe-3Al alloy was delivered in the shape of forgings of thickness 30 mm taken from one casting. The chemical composition of the examined alloy is shown in Ta-

* INSTITUTE OF MATERIALS SCIENCE, CRACOW UNIVERSITY OF TECHNOLOGY, AL. JANA PAWŁA II 37, 31-864 KRAKÓW, POLAND

ble 1. The heat and mechanical treatment was performed in two stages. The preliminary deformation was carried out in the β- range at the temperature of 900°C. The final stage of forging took place after cooling down to 750°C in the range of α and β-phases existence. The heat treatment consisted in annealing the forgings for an hour at 760°C followed by water cooling and ageing for 8 hrs at 480°C. As a result, the alloy revealed a bi-modal structure with spheroid precipitates of the α-phase in the β phase.

In order to establish the β-transus temperature, dilatometric examinations were performed in Ar atmosphere using NETZSCH TASC 414/2W instrument. The analysis was carried out on cylinder specimens of 4 mm in diameter and 25 mm in length. The samples were heated up to temperature 900°C at rate 10°C/min, held at that temperature for 15 min and cooled at rate 10°C/min. The temperature of β transformation was found to be 828°C. The heat treatment of the alloy was carried out in a tubular furnace Nabertherm P330 in an Ar protective atmosphere following two schemes shown in Fig. 1.

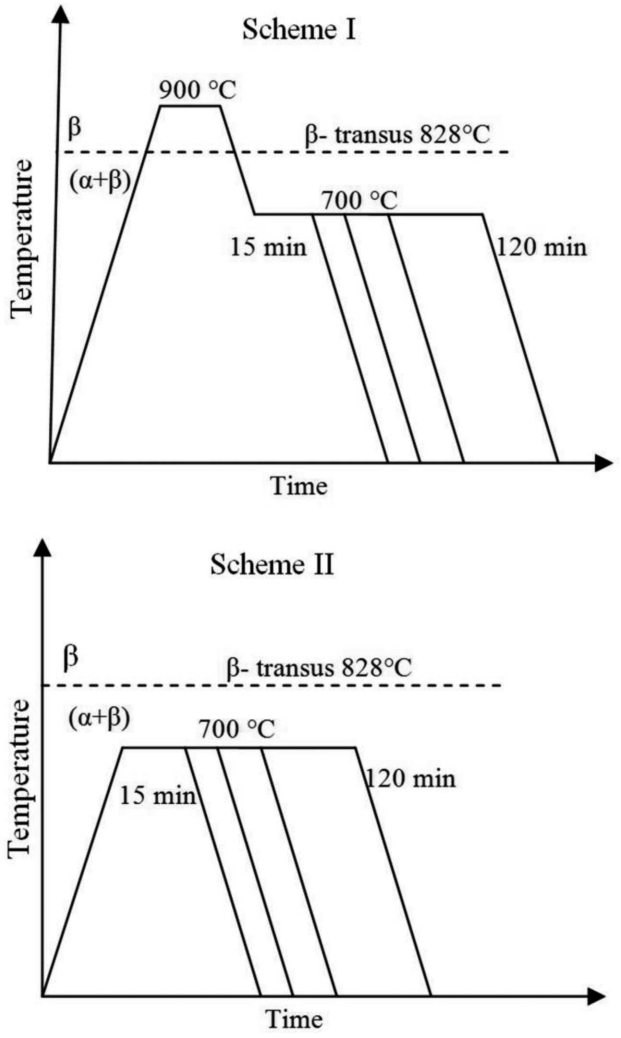

Fig. 1. Schemes of heat treatment

According to scheme I $\beta + (\alpha + \beta)$, an initial heating up to 900°C was applied at rate 10°C/min, followed by annealing for 20 min. Next, the sample was cooled with the furnace at rate 10°C/min. down to temperature 700°C, annealed for 15, 30, 60 and 120 min followed by water cooling (Fig. 1a).

Scheme II ($\alpha+\beta$) consisted in heating up to 700°C at rate 10°C/min. and annealing for 15, 30, 60 and 120 min, and then water quenched (Fig. 1b). The samples prepared in such a way were next subjected to microscopic observation, stereological analysis and mechanical testing.

Microstructural observations were performed using optical microscope NIKON ME 60 and scanning microscope JOEL JSM5510LV. The samples were chemically etched in a solution containing 10 ml HNO_3 + 20 ml HF + 20 ml glycerin. The stereological calculations of α-phase volume fraction were realized using ImageJ software at the total analysis surface of 1 mm^2. The hardness was examined with the use of Vickers tester at the load of 30 kg. The static tensile test was carried out on MTS Criterion Model 43 tensile machine at ambient temperature. Two cylinder samples 5 mm in diameter and 25 mm long taken in the longitudinal direction were prepared for each measuring point. Impact strength tests were done on standard samples of Charpy V type at room temperature using a percussive hammer of Alpha type at initial energy 300 J.

TABLE 1
Chemical composition of Ti-10V-2Fe-3Al alloy (wt.%)

Material	V	Al	Fe	O	N	C	Ti
Ti-10V-2Fe-3Al	9.9	2.9	1.9	0.13	0.007	0.02	bal.

3. Results

3.1. Microstructure

The alloy in the initial state revealed a bi-modal structure with distinctly elongated primary grains of the β-phase, which appeared as a result of the plastic deformation in the $(\alpha + \beta)$ range (Fig. 2a, b).

The basic objective of the heat treatments was to induce the microstructure of different morphologies and different α-phase volume fractions in the examined titanium alloy. To do so, two schemes of heat treatment were proposed. The scheme I brought about the appearance of needle-like α-phase (Fig. 3a-d). Annealing above the temperature of β transformation led to the recrystallization of deformed primary β-phase grains. It was observed, that prolonging the annealing time caused the increase of volume fraction of the α-phase.

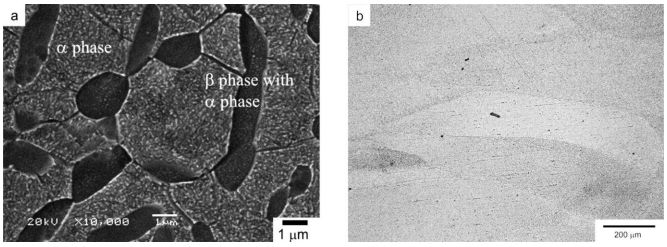

Fig. 2. SEM and optical micrographs of bi-modal structure in initial state

In the case of scheme II ($\alpha+\beta$) the α-phase had a globular form apart from the primary structure of deformed β-phase grains (Fig. 4a, b). The only exception was the specimen

annealed for 120 min, in which the beginning of recovery processes of the β-phase grains was observed (Fig. 4 c, d). In the range of analysed annealing times, slight differences in the α-phase morphology were registered. The extension of the time led to the change of shape from globular to elongated one (Fig. 4). In order to confirm the changes of volume fraction of the α-phase the stereological measurements were performed. Fig. 5 presents particular steps of analysis and the way of α-phase determination. The results of quantitative measurements are shown in the form of volume fraction V_v in Table 2. In the case of annealing in range $\beta + (\alpha + \beta)$ (regime I) a systematic increase of α-phase volume fraction can be observed from 17.8% after 15min up to 68.2% for 120 min. A different course was observed for scheme II ($\alpha + \beta$). The prolongation of annealing time resulted in a slow, but systematic decrease of the α-phase volume fraction from e.g. 58.3% to 50.9% after 15 and 120 min, respectively.

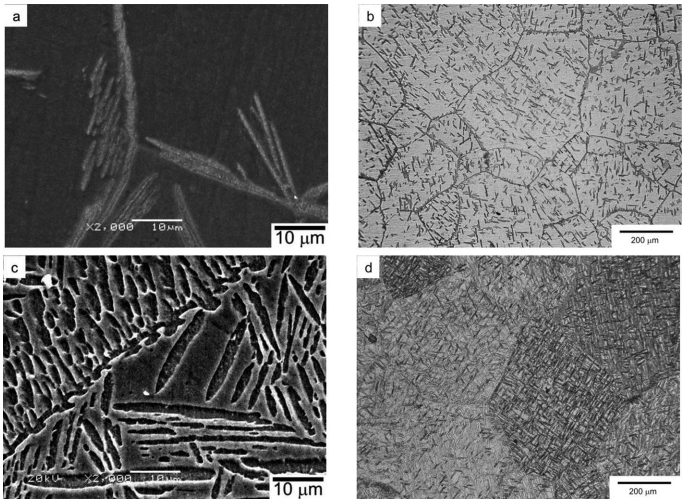

Fig. 3. SEM and optical micrographs of specimens after first scheme of heat treatment: a, b) acicular α phase in β matrix (900/700°C 15 min.), c, d) acicular α phase and β matrix (900/700°C 120 min.)

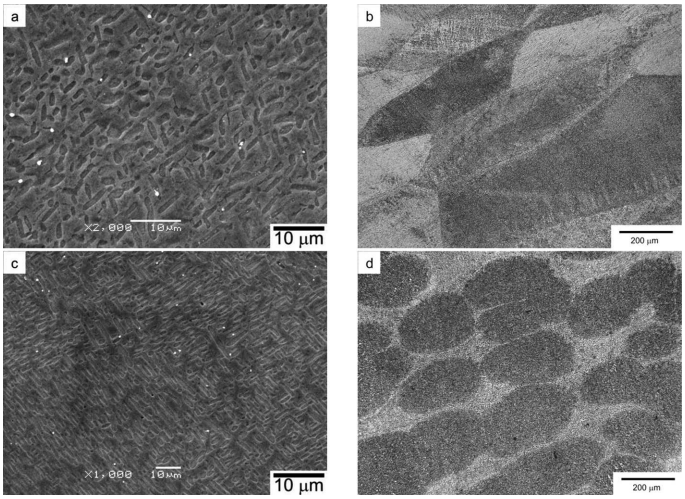

Fig. 4. SEM and optical micrographs of specimens after second scheme of heat treatment: a, b) globular α phase in β matrix (900/700°C 15 min.), c, d) globular and rod-like α phase and β matrix. The recovery processes of microstructure can be observed (900/700°C 120 min.)

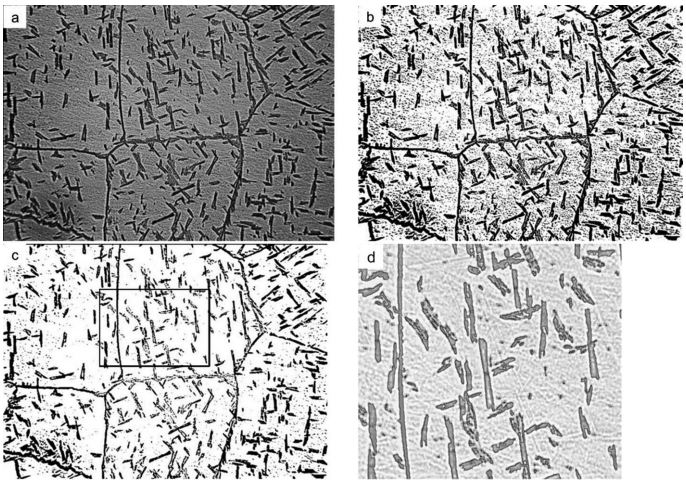

Fig. 5. The next steps lead to the calculation of the volume fraction of the phase α: a) micrograph of the initial, b) micrograph of the binarization c) image after dilation, closing, erosion and removal of noise, d) sample image after extracting of the α phase

TABLE 2

The volume fraction of α phase as a function of heat treatment

Temperature domain	Times of soaking	Morphology and volume fraction of α phase
$\beta + (\alpha + \beta)$	15 min.	acicular: ~17,7%
	30 min.	acicular: ~48,6%
	60 min.	acicular: ~62,9%
	120 min.	acicular: ~68,2%
$(\alpha + \beta)$	15 min.	globular: ~58,3%
	30 min	globular: ~53,7%
	60 min.	globular: ~51,5
	120 min.	globular: ~50,9

4. Mechanical properties

The results of mechanical property measurements are collected in Table 3. The increase of hardness and the Charpy V-notch impact energy can be observed together with the growth of annealing time in the case of scheme I $\beta + (\alpha + \beta)$. The lowest impact strength of 61 J was recorded after 15-min annealing, while the highest one of 86 J after 120 min. The elongation EL of the sample during tension test tended to decrease together with prolonging annealing time. The occurrence of strain induced martensitic transformation, (SIM) could be visible on tensile curves for scheme I after 15- and 30-min annealing (Fig. 6a). The phenomenon of SIM transformation was responsible for the appearance of second yield point, which can be determined according to the scheme presented in Fig. 6a. The prolonged time of annealing up to 60 min resulted in the decay of the SIM transformation.

The decrease of hardness together with lengthening of annealing time was observed when regime II ($\alpha + \beta$) was applied. A similar course was obtained for the measurements of impact energy, in which the lowest value of 51 J was recorded for the time of 60 min. The breaking force grew again to 88 J

for the sample annealed for 120 min, while between 15 and 60 min elongation was constant. The increase of elongation occurred after annealing for 120 min. In the case of YS and UTS these parameters were growing with time up to 60 min and then fell.

TABLE 3
Mechanical properties of titanium Ti-10V-2Fe-3Al alloy after different heat treatments

Temperature domain	Times of soaking	HV 30	Impact energy	EL	$YS_{0,2}$/ $YS_{0,2SIM}$	UTS
			[J]	[%]	[MPa]	[MPa]
β +(α + β)	15 min.	266	61	19,0	418 / 836	880
	30 min.	287	73	17,8	458 /841	873
	60 min.	289	84	12,2	772 / -	820
	120 min.	330	86	13,2	797 / -	824
(α + β)	15 min.	321	72	12,2	826 / -	844
	30 min.	307	64	12,3	842 / -	882
	60 min.	309	51	12,2	853 / -	883
	120 min.	312	88	14,0	828 / -	838

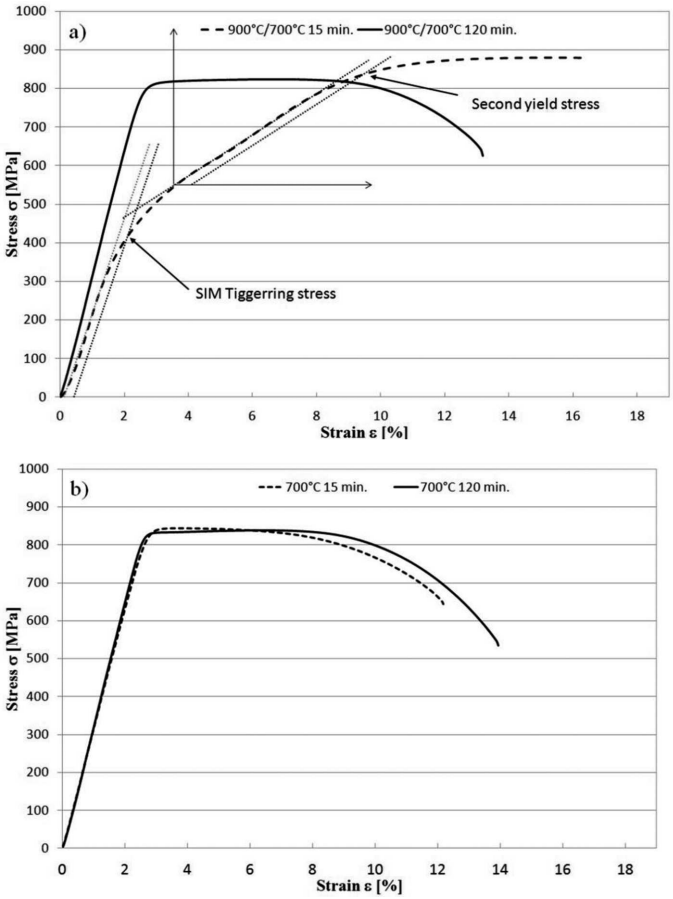

Fig. 6. Stress-strain curves as a function of heat treatment: a) curves of acicular α phase. The graph shows the method of determining SIM triggering stress and the second yield stress, b) curves for globular α phase after 15 and 120 min

5. Discussion

The Ti alloy of the Ti-10V-2Fe-3Al type after plastic deformation followed by supersaturation and ageing had a bi-modal structure consisted of areas of the α-phase and elongated grains of the β-phase, inside which fine particles of the α-phase were visible (Fig. 2).

The regimes of heat treatment allowed obtaining different morphology of the α-phase, while annealing time affected its volume fraction. The initial heating up to 900°C in procedure I led to the dissolution of α-phase and the recrystallization of β-phase grains. The following cooling below the temperature of β-phase transformation resulted in the beginning of precipitation of needle-like α-phase (Fig. 3 a-d). The volume fraction of the forming phase depended on annealing time. The increase of volume fraction of the α-phase brought about the increase of hardness and yield point. In the case of samples annealed for 15 and 30 min, whose volume fraction was below 50%, the occurrence of strain induced martensitic transformation (SIM) was observed, which is in accordance with the results reported in paper [6]. The phenomenon of SIM led to the hardening of the β matrix with the α'-phase appearing during deformation process, which was the reason for the increase of strength [6, 13-14]. The samples annealed for 15 and 30 min revealed the second yield point $YS_{0,2SIM}$ to be 836 and 841 MPa, respectively. The resistance to cracking measured with impact strength technique increased along with the increase of α-phase volume fraction at simultaneous decrease of elongation EL. It can be explained with the α-phase morphology of needles inclined at random angles, which during decohesion process became obstacles for crack proceeding and probably induced the change of cracking way. The decrease of elongation resulted from the growth of α-phase volume fraction, which crystallizes in a hexagonal system and has a limited ability to plastic deformation. The highest tensile strength of 880 and 873 MPa was obtained after annealing for 15 and 30 min, respectively. Lower UTS values of 820 and 824 MPa for 60 and 120 min, respectively should be bound with the lack of SIM transformation, which contributed to the alloy strengthening through the formation of α'-phase [6, 13-14].

The application of procedure II resulted in slight differences in the α-phase amount of globular morphology (Fig. 4 a-d), which might suggest, that the alloy was close to the equilibrium state. The morphology changed from the globular into rod-like shape of the α-phase, the volume fraction of which was above 50%, thus explaining the lack of SIM transformation occurrence. The mechanical properties did not change much, due to small difference in the α-phase content. The registered increase of the yield point resulted from the rise of the β-phase amount of higher strength. Similarly, the observed decrease of impact strain was due to the decrease of the α-phase amount That could be also bound with the change of shape of the α-phase, which together with the prolongation of the annealing time acquired the rod-like shape. The primary structure of the β-phase grains was preserved in the samples annealed for 60 min. The 120-min-annealing time induced the generation of recovery processes of the β-grains (Fig. 4d), which resulted in the decrease of strength and increase of ductility as well as impact strength.

6. Conclusions

1. The mode of heat treatment affected the morphology of the α-phase. The preliminary annealing above the temperature of the β transformation (according to scheme I) brought about the formation of acicular particles of the α-phase.
2. Controlling the time of annealing significantly affected the volume fraction of α-phase in the case of scheme I.
3. The annealing time did not influence the volume fraction of α-phase when regime II was used, however it did affect the morphology of particles, whose shape changed from globular into needle-like one.
4. Annealing for 120 min according to scheme II led to the appearance of structure recovery processes.
5. The occurrence of strain-induced martensite transformation SIM strengthened the alloy, heat treated according to regime I, resulting in higher strength of material annealed for 15 and 30 min.

REFERENCES

[1] G.T. Terlinde, T.W. Duerig, J.C. Williams, Metall. Mater. Trans. **A 14**, 2101-2115 (1983).

[2] T.W. Duerig, J. Albrecht, D. Richer, P. Fischer, Acta Metall. **30**, 2161-2172 (1982).

[3] R. Dąbrowski, The kinetics of phase transformations during continuous cooling of Ti6A|4V alloy from the diphase $\alpha_{+\beta range}$, Arch. Metal. Mater. **56**, 217-221 (2011).

[4] R. Dąbrowski, The kinetics of phase transformations during continuous cooling of Ti6A|4V alloy from the single-phase *βrange*, Arch. Metal. Mater. **56**, 703-707 (2011).

[5] R.R. Boyer, R.D. Brigs, Journal of Materials Engineering and Performance **14**(6), 681-685 (2005).

[6] C. Li, X. Wu, J.H. Chen, S. van der Zwaag, Materials Science and Engineering A **528**, 5854-5860 (2011).

[7] M. Jackson, R. Dashwood, L. Christodoulou, H. Flower, Metallurgical and Materials Transactions A **36A**, 1317-1327 (2005).

[8] L. Zhou, G. Liu, X.L. Ma, K. Lu, Acta Mater. **56**, 78-87 (2008).

[9] P.J. Apps, J.R. Bowen, P.B. Prangnell, Acta Mater. **51**, 2811-2822 (2003).

[10] I. Gutierrez-Urrutia, M.A. Munoz-Morris, D.G. Morris, Mater. Sci. Eng. A **394**, 399-410 (2005).

[11] A. Paradkar, V. Kumar, S.V. Kamat, A.K. Gogia, B.P. Kashyap, Materials Science and Engineering A **486**, 273-282 (2008).

[12] A. Bhattacharjee, V.K. Varma, S.V. Kamat, A.K. Gogia, S. Bhargava, Metallurgical and Materials Transaction **37A**, 1423-1433 (2006).

[13] W. Chen, Q. Sun, L. Xiao, J. Sun, Materials Science and Engineering A **527**, 7225-7234 (2010).

[14] A. Bhattacharjee, S. Bhargava, V.K. Varma, S.V. Kamat, A.K. Gogia, Scripta Materialia **53**, 195-200 (2005).

[15] A. Paradkar, S.V. Kamat, A.K. Gogia, B.P. Kashyap, Materials Science and Engineering A **491**, 390-396 (2008).

Received: 20 January 2014.